Egyptian Geophysical Society
EGS Journal, Vol. 8, No. 1, 117-130 (2010)

Vs(30), NEHRP SITE CLASSES AND SITE AMPLIFICATION FACTOR ESTIMATIONS IN THE KANTO REGION, CENTRAL JAPAN

M.M.F. Shokry[(1)] and N. Hirata[(2)]
1- Department of Geophysics, Faculty of Science, Ain Shams University, Cairo, Egypt, 11566
2- Earthquake Prediction Research Centre, Earthquake Research Institute, Tokyo University, Japan

حساب كل من سرعة القص لطبقة ٣٠ متر السطحية ((Vs(30))، تصنيف المواقع باستخدام نظام (NEHRP)، بالإضافة إلي حساب معامل التكبير لمنطقة الكانتو، بوسط اليابان

الخلاصــة: تم استخدام المعلومات المتاحة والخاصة بشبكتى رصد الزلازل (*K-NET and KiK-net*) بالإضافة إلى أنه تم الاستعانة أيضا بعدد من تسجيلات الآبار الضحلة والعميقة والتى تصل إلى صخور القاعدة فى بعض الآبار، وذلك من أجل عمل تقييم إقليمى لمنطقة الكانتو. ولقد تم حساب السرعة المتوسطة للطبقة السطحية بسمك ٣٠ متر (*(Vs(30)*) وذلك من أجل تصنيف المنطقة من حيث قابلية المنطقة لتكبير الموجات الزلزالية من عدمه، وذلك اعتمادا على نظام التصنيف العالمى (NEHRP) لتصنيف المواقع. ولكن فى كثير من الأوقات لم نتمكن من حساب قيمة (*(Vs(30)*) وخاصة لشبكة (*K-NET*)، و ذلك لأن المعلومات المتاحة للآبار المستخدمة من هذه الشبكة لا تصل فى كثير من الأحيان إلى عمق ٣٠ متر. ولحل هذه المشكلة حتى نتمكن من حساب قيمة (*(Vs(30)*) تم استخدام عدد من الطرق الرياضية، حيث شملت هذه الطرق طريقتين أساسيتين تم من خلالهما استخدام المعلومات المتاحة من عدد (٥٨) بئر موزعة بانتظام بشبكة (*KiK-net*)، وذلك للوصول إلى نموذج للسرعة حتى عمق ٣٠ متر. ومن أسهل الطرق المستخدمة، الطريقة التى أفترضت أن سرعة الطبقة الأخيرة امتدت حتى نهاية البئر حتى عمق ٣٠ متر وكانت هذه الطريقة هى أكثر الطرق دقة مقارنة بالطريقة الأخرى التى تم من خلالها عمل مقارنات بين (*(Vs(30)*) والسرعات للطبقات الضحلة بطول البئر. ولقد أوضحت نتائج الطرق المستخدمة أن نسبة المواقع التى لم تتطابق مع التصنيف الأصلى للموقع هى نسبة لم تتعدى ١٠%. أيضا تم حساب معامل التكبير لمنطقة الكانتو بالإضافة إلى أنه تم اختيار زلزالين ممثليين لمنطقة الكانتو وتم من خلالهما عمل مقارنة بين قيمة عجلة الجاذبية الأرضية (PGA) العظمة المسجلة والمستنتجة من بعض العلاقات الرياضية. وأظهرت أيضا هذه الدراسة مدى أهمية الاستفادة من المعلومات المتاحة والمتوفرة والخاصة بشبكتى رصد الزلازل (*K-NET and KiK-net*) على موقع الإنترنت.

ABSTRACT: *Data from K-NET and KiK-net, together with shallow/deep borehole recordings obtained for the pre-Tertiary basement, were used to evaluate regional site effects in the Kanto region. The average velocity to 30 m depth (Vs(30)) was calculated, so as to classify sites to predict their potential for amplifying seismic shaking, depending on the NEHRP Site Class System. In many cases, however, shallow shear-wave velocity data for K-NET, from which Vs(30) can be computed, do not extend to 30 m depth. In order to use the data for these cases, a method to extrapolate the velocities must be devised. Two such methods are described herein and illustrated using data from 58 boreholes of KiK-net, for which the velocity model extends to at least 30 m. The simplest method assumes that, the lowermost velocity extends to 30 m results in significantly less bias than methods using correlations between shallow velocities and Vs(30). In addition, for all methods, the percent of misclassified sites was generally less than 10%. The site amplification factor was calculated in the Kanto region. Also, the maximum Peak Ground Acceleration (PGA) for two selected earthquakes was estimated and compared with the actual PGA. This study also emphasises the usefulness of the K-NET and KiK-net data currently available on the internet.*

INTRODUCTION

The Kanto region, which includes Tokyo, Central Japan, is the centre of political and economic activities in Japan and contains one-third of Japan`s population. The Kanto region is a geographical area located on Honshu, the largest island of Japan. Its boundary is nearly the same as that of the Kanto plain. The region consists of seven prefectures: Gunma, Tochigi, Ibaraki, Saitama, Tokyo, Chiba and Kanagawa. It is one of the most active seismic zones in the world, and many disastrous earthquakes have occurred in and around the region. Several types of earthquake mechanisms are observed in this region, because of the complicated tectonic structures caused by the complex relative movements of the Philippine Sea Plate, the Pacific Plate, and the North American Plate (Okada and Kasahara, 1990; and Ishida, 1992). Recently, large-scale buildings, such as tall skyscrapers and big oil and gas tanks, have become significantly more common in the metropolitan area. These have long natural periods, so they should respond to long-period ground motions, that are affected by the sedimentary basin structure and the geophysical properties of the bedrock, basement rocks and sediments. More than 3000 meters of sediments underlie the Kanto region, resting on the pre-Tertiary basement, which is similar in structure to many metropolitan areas around the world. Previous interpretations, based on geophysical exploration, show that the base of this sedimentary basin is smooth (Komazawa and Hasegawa, 1988; Koketsu and Higashi, 1992; Suzuki, 2002; and Yamanaka and Yamada, 2002 & 2005;) (Fig. 1).

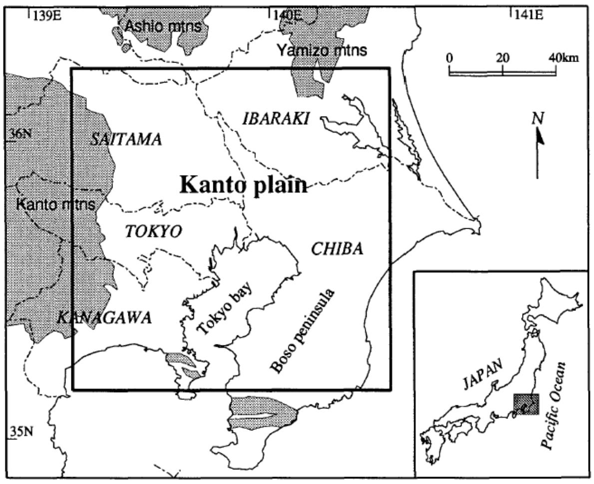

Fig. (1): Index map showing the location of the Kanto Region and its geographical and geological setting. The pre-Tertiary basement outcrops are shown in the shaded areas. The rectangle drawn with thick lines indicates the 120 × 120 km target area of the Kanto Region. The capital letters in italics designate the names of the prefectures in the Kanto Region.

An accurate evaluation of the ground amplification characteristics requires detailed soil profile information, such as shear-wave velocity structures. An approximate estimate of ground amplification is possible if given the shear-wave velocity of the surface layer (Borcherdt and Gibss, 1976), and the amplification of strong ground motion, such as peak ground velocity, is correlated with the average shear-wave velocity from the ground surface to a certain depth (Joyner and Fumal, 1984; and Midorikawa et al., 1994). In the U.S., the average shear-wave velocity of the upper 30 m of ground (Vs(30)) is used to classify soil, according to the seismic code (e.g., Dobry et al., 2000; and BSSC, 2001 & 2003) and to estimate losses. The site classes estimated from shallow shear-wave velocity models are also important in deriving strong-motion prediction equations (e.g., Boore et al., 1997), in constructing maps of National Earthquake Hazard Reduction Program (NEHRP) site classes (e.g., Wills et al., 2000), and in applying building codes to specific sites.

The ultimate goal of the present study is to estimate the NEHRP site classes, peak ground acceleration and peak ground velocity in order to predict their potential to amplify seismic shaking in the Kanto region. In the study area, our analysis of the down-hole shear-wave velocity values could tangibly delineate the soil/bedrock layering.

DATA

To implement our study, we needed data from a systematic network of strong-motion observations. The National Research Institute for Earth Science and Disaster Prevention (NIED) constructed a strong-motion network, the K-NET (Kinoshita, 1998), followed by the construction of a high sensitivity digital strong-motion seismograph network (KiK-net) across all of Japan. The data from the K-NET and KiK-net are now available on the internet. In this study, we used the soil conditions information employed in the Kanto region study from the K-NET and KiK-net sites data released on the internet.

We used the information regarding the down-hole soil conditions of the K-NET and KiK-net station sites, which are well distributed in the Kanto region, with a station-to-station distance of about 25 km. K-NET sites data contain shallow down-hole soil condition, information (P-wave and S-wave velocities) for 110 stations. The down-hole measurements are between 10 to 20 m in depth. However, the KiK-net sites data contain deep down-hole soil measurements for 58 stations between about 100 and 2,000 m in depth (Fig. 2).

$V_s(30)$ Calculation And NEHRP Site Classes

Many measurements of near-surface shear-wave velocity, however, do not reach 30 m in depth, such as in the case of the shear-wave velocities at the K-NET sites, which are measured between depths of 10 and 20 m. We compared several ways of estimating Vs(30) from velocity models, that do not reach 30 m (the models can be determined using either invasive or non-invasive methods). The simplest method assumes that, the lowermost velocity of the model extends to 30 m; the other methods use correlations between shallow velocities and Vs(30) (Boore, 2004). According to the best distribution of the site locations of both K-NET and KiK-net and in order to use as much data as possible for our study, to calculate Vs(30) for all sites to obtain a final NEHRP site classes map of the Kanto region, the following disciplines should be studied.

Vs(d) Calculation and NEHRP Site Classes of KiK-net

First, the average shear-wave velocity in the upper 30 m [Vs(30)] was calculated and weighted by the travel time of the shear-wave, for all PS logging data for KiK-net in the Kanto region. For this calculation, we applied the criteria of the Vs(30) calculation described by Fujimoto and Midorikawa (2003). NEHRP classes were determined by Vs(30) for KiK-net, as indicated in Table 1 (Fig. 3), in which the analysis was dominated by NEHRP classes B to E. In the same way, we applied the criteria of the Vs(20) calculation of Fujimoto and Midorikawa, (2003), but to 20 m depth, and compare it with Vs(30) (Fig. 4).

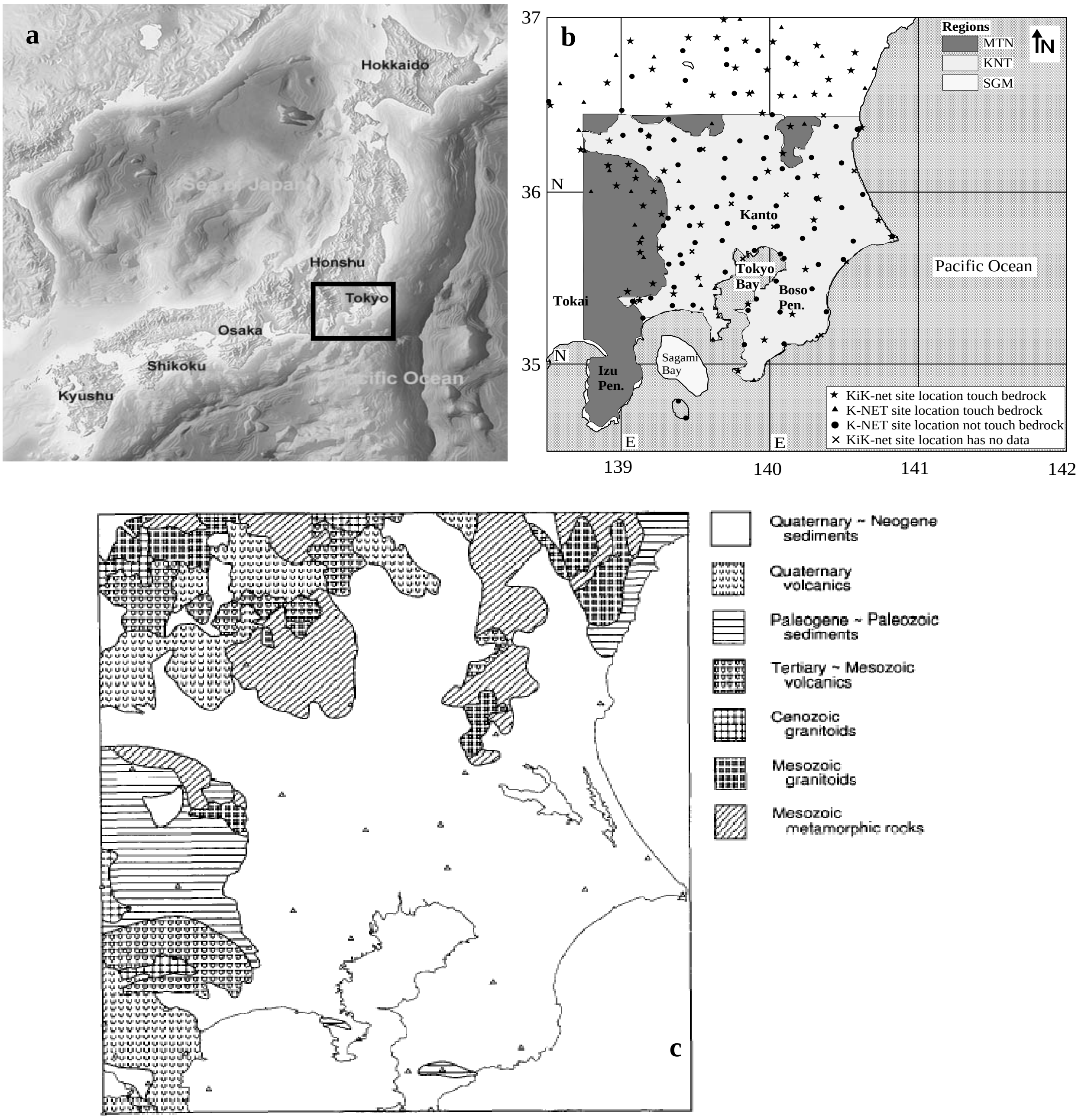

Fig. (2): a: Regional topographic map of Japan showing the finite difference (FD) grid area (black rectangle) of the Kanto district, including the Tokyo metropolitan area. Seafloor topography around Japan is also shown (Smith and Sandwell, 1997). b: Map showing the whole FD grid area and stations included in this study. Stars, triangles, circles, and crosses indicate the KiK-net site locations that reached bedrock, the K-NET site locations that reached bedrock, the K-NET site locations that did not reach bedrock, and the KiK-net site locations lacking data, respectively. The regions displayed in dark, medium, and light grey are the mountain region (MTN), the Kanto basin region (KNT), and the Sagami basin region (SGM) along the Sagami Trough, respectively. c: Geological map of the area surrounding the Kanto region reproduced from the Geological Survey of Japan (1992).

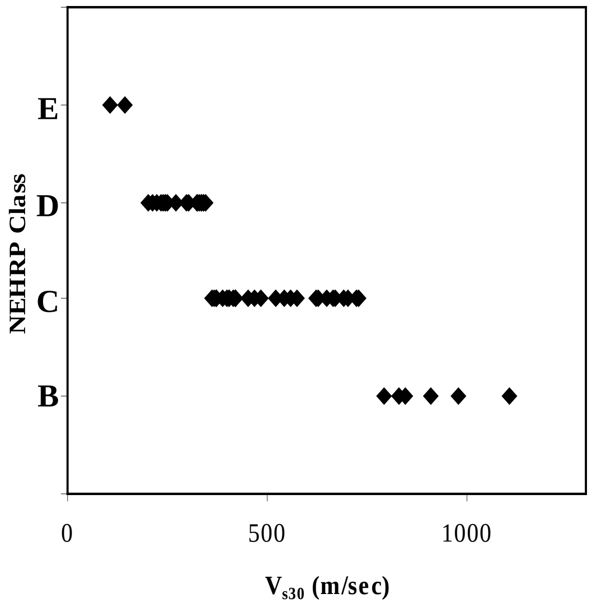

Fig (3): NEHRP site classes in terms of $V_s(30)$ for the KiK-net sites in the Kanto region.

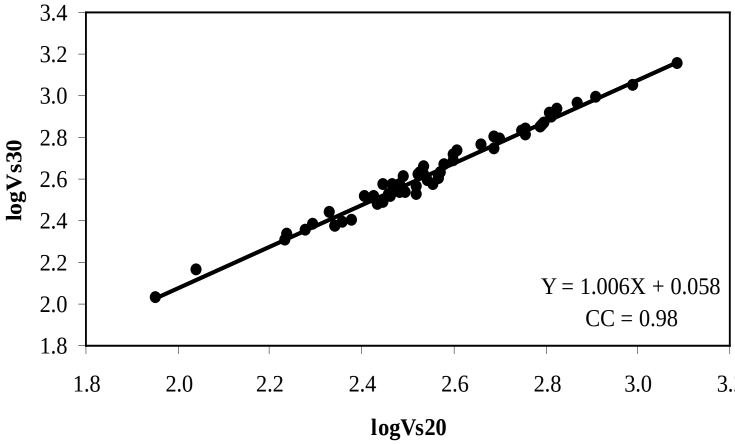

Fig (4): Relationship between average shear-wave velocity $V_s(20)$ extending to 20 m and average shear-wave velocity $V_s(30)$ extending to 30 m.

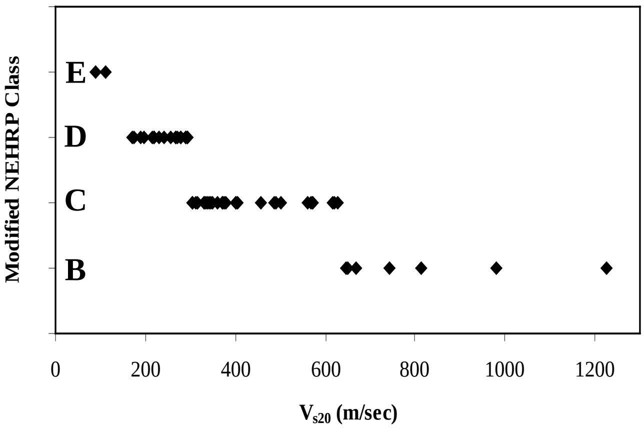

Fig (5): Modified NEHRP site classes in terms of $V_s(20)$ for the KiK-net sites in the Kanto region.

The coefficient of correlation was as high as 0.98, so the association between Vs(30) and Vs(20) was basically an acceptable linear relationship and matched with the derived correlation equation between Vs(20) and Vs(30) described by Kanno et al. (2006) from the results of PS-logging at KiK-net sites. According to this linear relationship, the NEHRP site classes were modified to new classes using Vs(20) of Table 1, and the analysis was dominated by the modified NEHRP classes B to E matching with NEHRP classes compared to Vs(30) (Fig. 5). However, 10% of the KiK-net sites in the Kanto region changed their site classes when Vs(20) was used in the NEHRP site classes instead of Vs(30).

Using the same set of KiK-net boreholes, for which the actual depths reached or exceeded 30 m, we found that the plots of Vs(30) against Vs(d) for a series of assumed depths (d) could be fit to a straight line. The scattering of these plots, however, increased with Vs(d). For this reason, a power-law relationship between Vs(30) and Vs(d) was assumed, for which a straight line can be fit to the logarithms of the quantities. Figure (6) shows examples for five assumed depths. The correlation was good, even for the shallowest depth considered herein (10 m). The velocity at the bottom of the model (Vs(d)) rather than the average velocity Vs(d) was also considered as a predictor variable, but the scatter was worse. Vs(d) has the advantage, however, that it can be used if shallower parts of the velocity model are missing, as is often the case with suspension log results.

Table 1. Definition of NEHRP Site Classes in Terms of Vs(30) and Vs(20), the Average Shear-Wave Velocity to 30 and 20 m, respectively.

Site description	NEHRP (ICC, 2006) Vs(30) dependent Range of Vs(30) (m/sec)	Site class	Modified NEHRP Vs(20) dependent Range of Vs(20) (m/sec)
Hard rock	1,500< s(30)	A	1,250< Vs(20)
Rock	760<Vs(30)≤ 1,500	B	640<Vs(20)≤1,250
Dense soil & soft rock	360<Vs(30)≤ 760	C	300<Vs(20)≤640
Stiff soil profile	180≤Vs(30)≤360	D	160≤Vs(20)≤300
Soft soil profile	Vs(30)<180	E	Vs(20) < 160

We considered the boreholes of KiK-net did not extend below 20 m in depth, and calculated Vs(30) by simulation, assuming that the shear-wave velocity at 20 m depth continues and can be extrapolated to 30 m depth (Fig. 7a). We also calculated Vs(30) by simulation, assuming a linear relation between the actual Vs(30) and Vs(20) obtained in Fig. (4). We then compared these results with the actual Vs(30) (Fig. 7b). The results showed that, both relationships exhibited slight dispersions and that, the coefficient of correlation was 0.99 in the case of Vs(30) calculated by simulation, assuming that the shear-wave velocity at 20 m depth continues to 30 m depth and equals 0.98 for Vs(30) calculated by simulation, assuming a linear relationship between the actual Vs(30) and Vs(20).

Vs(30) Calculation and NEHRP Site Classes of K-NET

For the data given from K-NET with depths less than 30 m, Vs(20) was calculated for the K-NET sites using the modified equation described by Fujimoto and Midorikawa (2003) to 20 m depth and compared with Vs(20) calculated for the KiK-net sites in Fig. (8). The coefficient of correlation was as high as 0.96, so the relationship between Vs(20) for the two kinds of nets used (K-NET and KiK-net) proved to be a basically acceptable linear relationship. Vs(30) for the K-NET sites was calculated by simulation, assuming that the shear-wave velocity of 20 m depth continues and can be extrapolated to 30 m depth, and Vs(30) was also calculated by simulation, assuming a linear relationship between the actual Vs(30) and Vs(20) obtained in Fig. (4). A linear relationship between the two types of results for Vs(30) was obtained and plotted with a correlation coefficient equal to 0.93 (Fig. 9). NEHRP classes were determined using the two types of estimated Vs(30) for K-NET, as indicated in Table 1 (Fig. 10), and the analysis was dominated by NEHRP classes C to E, except for two sites classified as class B when using Vs(30) calculated based on the linear relationship. In addition, for the two methods used to estimate Vs(30) at the K-NET sites, the percentage of sites misclassified or not matched was generally less than 10%. Based on these observations, we concluded that, we could approximate Vs(30) for those sites which have survey depths of less than 30 m and shear-wave velocity data in the upper 20 m by simulation, assuming that the shear-wave velocity at 20 m depth continues to 30 m depth with the same velocity gradient.

Vs(30) Calculation and NEHRP Site Classes for the Kanto Region

Vs(30) was calculated for all the K-NET and KiK-net sites in the Kanto region, as ranged between 91 and 1,433 m/sec (Fig. 11). This high shear-wave velocity was recorded only at two sites, the first at KiK-net site TCGH17 (with the maximum value) and the second at KiK-net site TKYH13 (with a shear velocity of 1,110 m/sec). If these two high values were omitted, the Vs(30) are ranged between 91 and 983 m/sec. The Vs(30) values in major plains are small, while the geomorphologic units with higher elevations towards the mountainous areas exhibit larger Vs(30) values (Matsuoka et al., 2006), as evidenced in the present study.

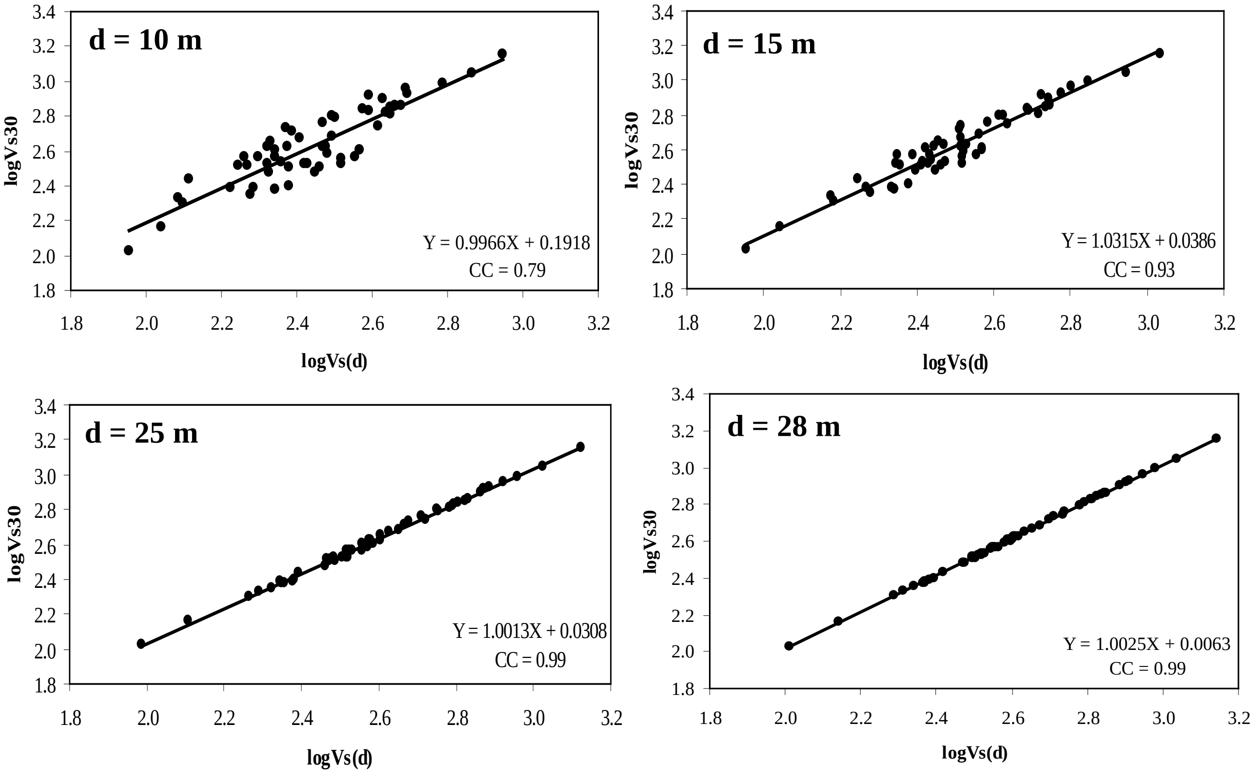

Fig (6): Straight line fit to log $V_s(30)$ as a function of log $V_s(d)$ for d = 10, 15, 25, and 28 m, with velocities in meters per seconds, for the KiK-net sites in the Kanto region.

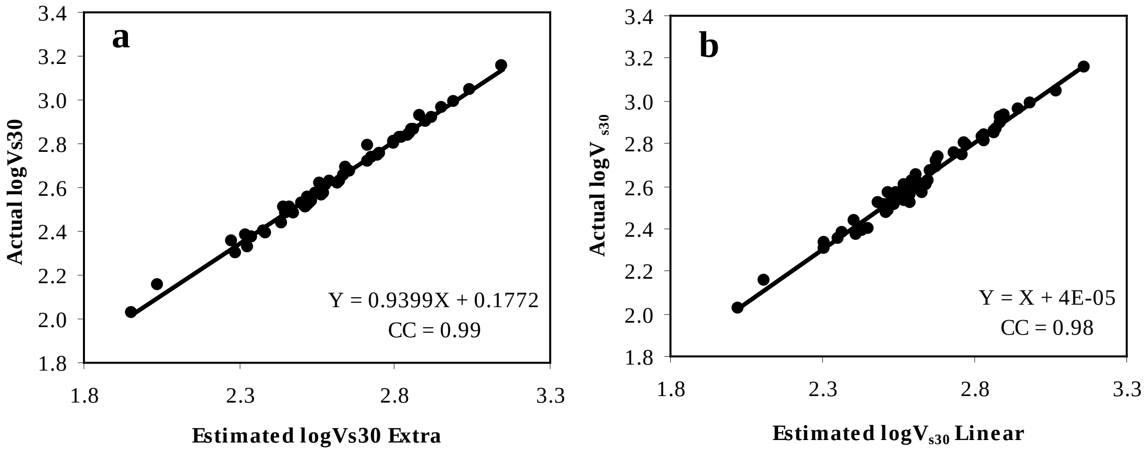

Fig (7): (a) Relationship between log average shear-wave velocity calculated on the assumption that the upper 20-meter layer extends to 30 m and the actual log average shear-wave velocity. (b) Relationship between log average shear-wave velocity calculated on the assumption that the upper 20-meter layer exists in a linear relationship extending to 30 m and the actual log average shear-wave velocity for the KiK-net sites in the Kanto region.

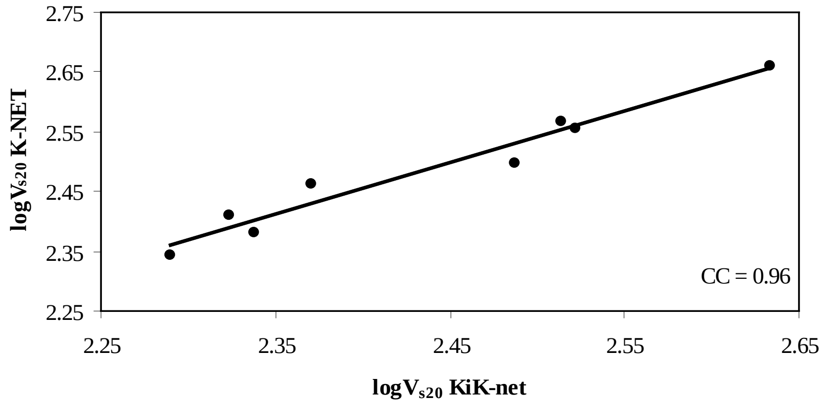

Fig (8): Relationship between the calculated log average shear-wave velocity $V_s(20)$ for KiK-net and K-NET.

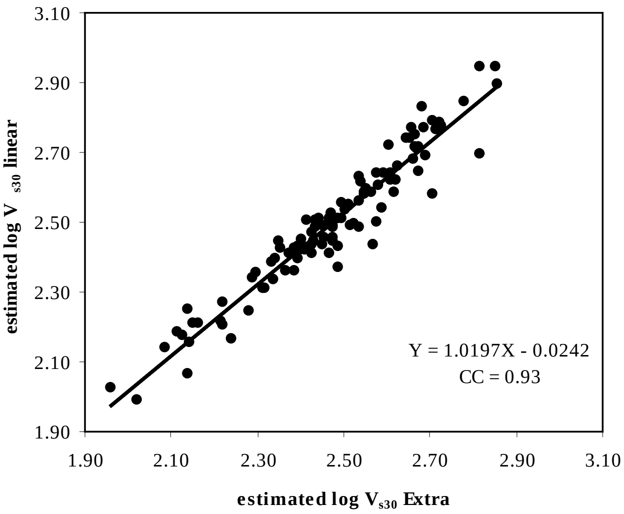

Fig (9): Relationship between the log average shear-wave velocity calculated on the assumption that the upper 20-meter layer extends to 30 m and the log average shear-wave velocity calculated on the assumption that the upper 20-meter layer exists in a linear relationship extending to 30 m for K-NET sites in the Kanto region. **Fig (9): Relationship between the log average shear-wave velocity calculated on the assumption that the upper 20-meter layer extends to 30 m and the log average shear-wave velocity calculated on the assumption that the upper 20-meter layer exists in a linear relationship extending to 30 m for K-NET sites in the Kanto region.**

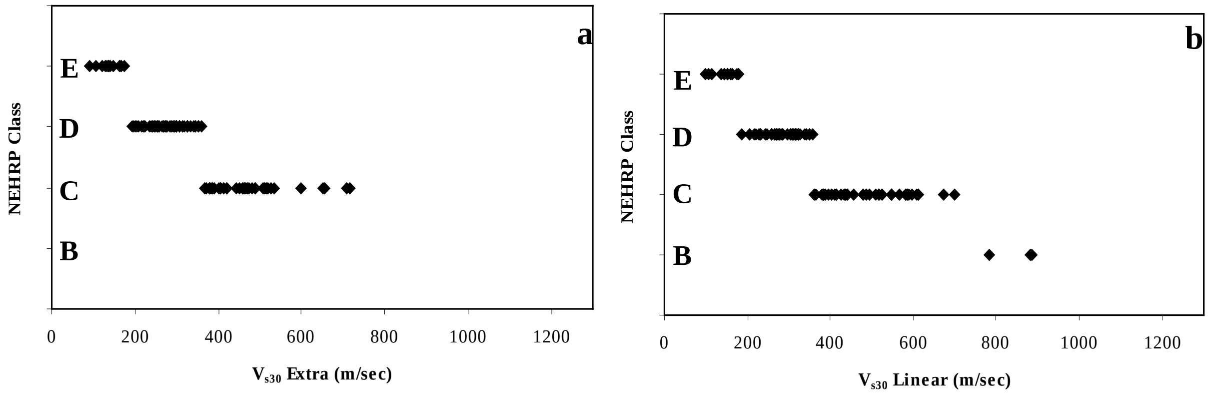

Fig (10): (a) NEHRP site classes in terms of $V_s(30)$Extra. (b) NEHRP site classes in terms of $V_s(30)$ Linear for K-NET sites in the Kanto region.

The NEHRP classes were determined for K-NET and KiK-net sites, as indicated in Table 1 (Fig. 12a), and the analysis was dominated by NEHRP classes B to E. The NEHRP classes lateral distribution (Fig. 12b) displayed four classes ranging from B to E, as indicated in Table 1. Classes B and C are related to rock and dense soil or soft rock materials, respectively, and generally match the mountainous areas to the north and north-western sides of the Kanto region. On the other hand, class D, which is related to stiff soil, is spread throughout most areas of the Kanto basin. The fourth class, E, is related to soft soil materials and appears as small isolated spots, the main one found near the intersection between longitude 140o and latitude 36o of the Kanto region, near other distinct regions on the eastern and western edges of the Boso peninsula. This class E may be related to the low average shear velocity recorded in these areas at KiK-net sites IBRH07 and IBRH10 and at K-NET sites CHB008, CHB009, CHB015, CHB016, CHB019, CHB020, KNG001, KNG009, KNG002, KNG013, SIT003, SIT008, SIT010, and SIT011 with shear-wave velocities ranging between 91 and 174 m/sec. These low values of average shear velocity may be due to the lithologic units recorded and described during the drilling process at the above-mentioned sites. These lithologic units varied between loose SAND layers (SPT < 10), loose SILT layers (SPT < 10), very soft to soft silty CLAY layers (SPT < 6), and organic soil layers (Peat).

Site Amplification Factor Estimation

The strong influence of near-surface geological conditions, in the form of sediment amplification or site response, has been apparent from the damage distributions of many destructive earthquakes. There are many factors that influence the way a site will respond to earthquake ground motion (Aki, 1988; Aki and Irikura, 1991; and Bard, 1994). For the engineering community, the site effect is often regarded as the influence of the upper 30 m. However, seismologists often think of surface waves generated at the boundary of a sedimentary basin (which may have dimensions of several kilometres) as a site effect. Therefore, it is important that, the meaning of site response be clearly defined. In order to prepare for an earthquake via seismic strengthening and seismic design of civil structures and buildings, evaluation of the intensity distribution of ground motion input is important. Fujimoto and Midorikawa (2006) derived an empirical relationship (Eq. 1) between the average shear-wave velocity (Vs30) of the ground and the site amplification factor (AF).

$$\text{Log (AF)} = -0.852 \log (\text{Vs30}/600) = 2.367 - 0.852 \log \text{Vs30} \pm 0.166 \quad (1)$$

Eq. 1 was used to calculate the site amplification factor for all sites of the K-NET and KiK-net in the Kanto region (Fig. 13b). The AF is ranged between 0.4 and 4.97. A high site amplification factor corresponds to those zones with relatively thick sedimentary thicknesses (Fig. 13a), relatively low values of average shear-wave velocity (Vs30) (Fig. 11), and low NEHRP site class orders (class D and E) (Fig. 12b). The site amplification factor values move from thick sediment zones with relatively high values to mountainous areas with relatively low values. For more detailed site amplification factor results, (Vs30) data at small interval spacings are needed.

Actual/Estimated Peak Ground Acceleration

One of the most important problems in earthquake engineering is how to predict the peak ground acceleration (PGA) of future earthquakes from the available past activity data for a specified site. In engineering applications, it is often necessary to estimate not only the PGA, but also the response spectrum as a parameter for design. We examined the attenuation characteristics of peak ground acceleration, based on strong motion recordings from eight earthquakes located in the Kanto region during the last 10 years (Fig. 14a). According to Seno et al. (1993 & 1996), the Eurasian and Okhotsk plates are bounded by the Itoigawa-Shizuoka tectonic line. The Pacific plate and the Philippine Sea plate subduct along the Japan trench and the Sagami-Suruga trough, respectively. The collision of the Izu-Ogasawara volcanic arc on the Philippine Sea plate with the central Honshu arc form a collision zone north of the Izu peninsula. The intersections of these plate boundaries form two triple-junctions: one is the inland junction located north of the Izu peninsula and the other is located far southeast off the Boso peninsula.

Figure 14b shows a vertical cross-section of the seismicity of the selected eight earthquakes used in this study beneath the Kanto-Tokai area and some composite focal mechanism solutions used from F-net. The composite focal mechanism solutions reflect normal faulting in the shallow parts and reverse faulting in the relatively deep parts. In contrast, beneath the Tokai area, the Philippine Sea plate seismic zones are relatively thin and simple, where the plate boundaries at shallow depths are aseismic and recognised as the currently locked interface, although the shallower border east of the Boso peninsula is not definite due to the low seismicity (Matsumura, 1997; and Noguchi, 2002).

We examined the attenuation characteristics of the actual PGA, based on strong motion recordings from eight earthquakes recorded by the distributed station of K-NET and KiK-net in the Kanto region (Fig. 15). The regression analysis revealed that, shallow earthquakes have a relatively low actual PGA compared with the deep earthquakes engineering applications. An attenuation relationship has been expressed as a mathematical function relating a strong-motion parameter (e.g., PGA & PGV) to parameters characterising the earthquake magnitude, propagation medium, local site geology, and engineering structure (Campbell, 1985).

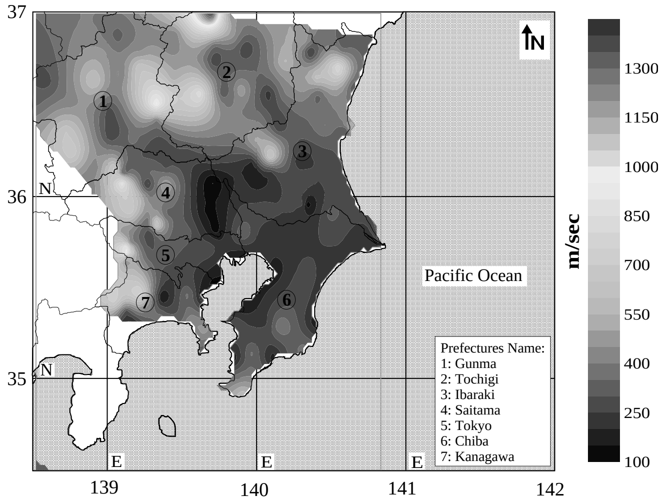

Fig (11): $V_s(30)$ distribution estimated by the K-NET and KiK-net sites for the Kanto Region.

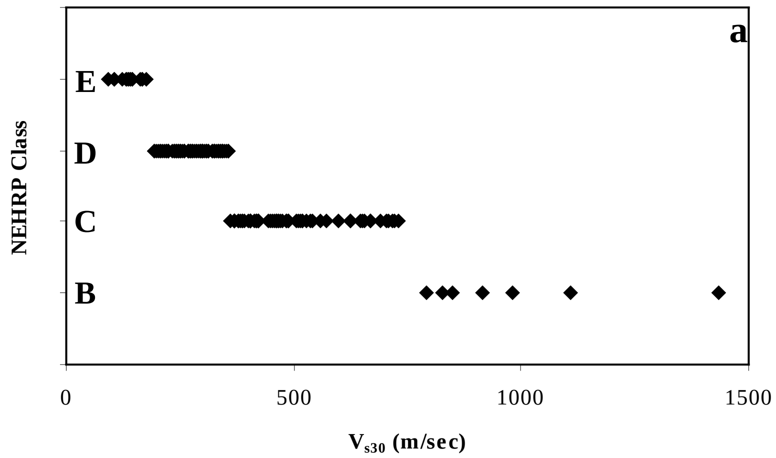

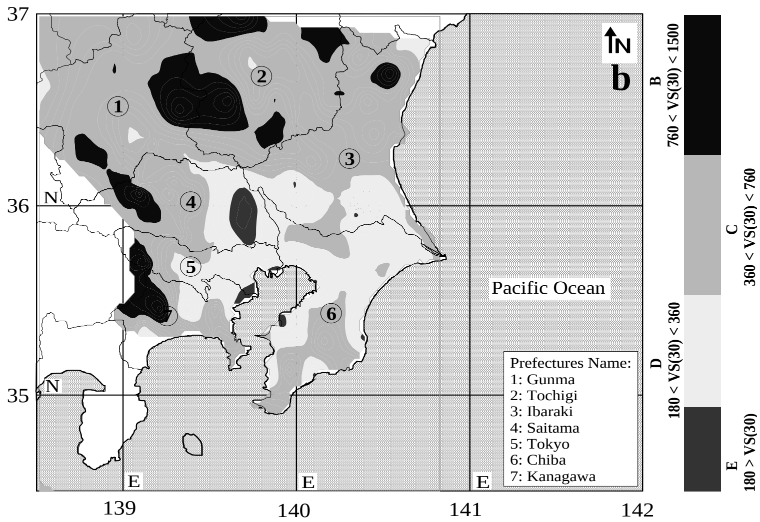

Fig (12): (a) NEHRP site classes in terms of $V_s(30)$. (b) Contour map illustrating the NEHRP site class lateral distribution for the K-NET and KiK-net sites in the Kanto region.

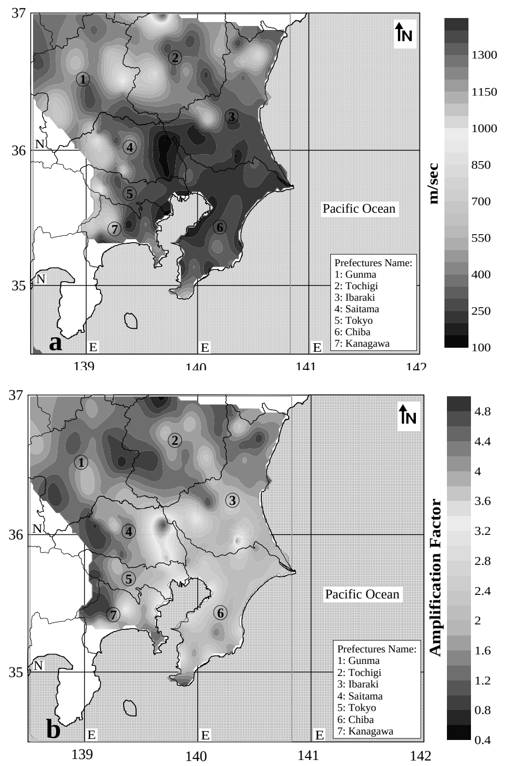

Fig (13): (a) Contour map illustrating the $V_s(30)$ distribution. (b) Site amplification factor distribution estimated by the K-NET and KiK-net sites for the Kanto Region.

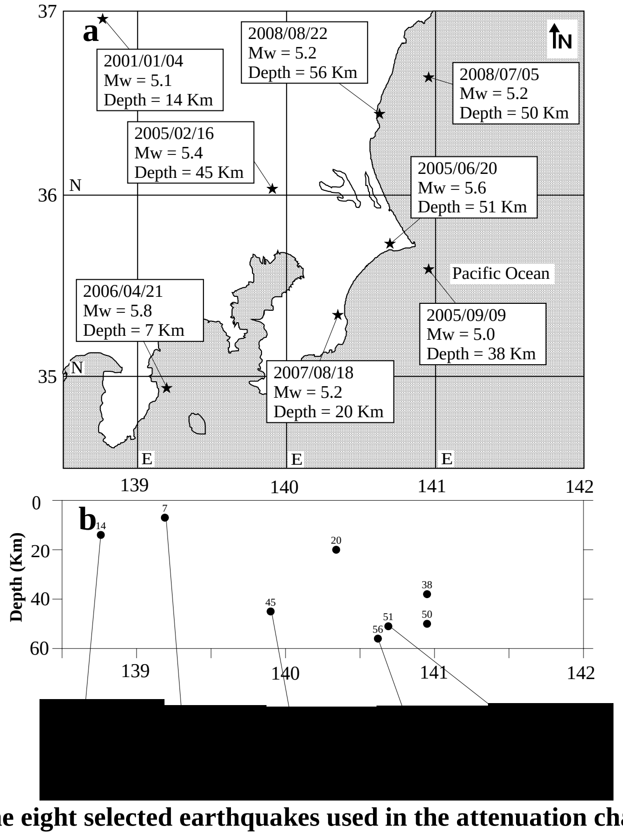

Fig (14): (a) The eight selected earthquakes used in the attenuation characterisation. (b) Vertical cross-section of the seismicity of the selected eight earthquakes and some composite focal mechanism solutions (F-net) at shallow and relatively deep depths.

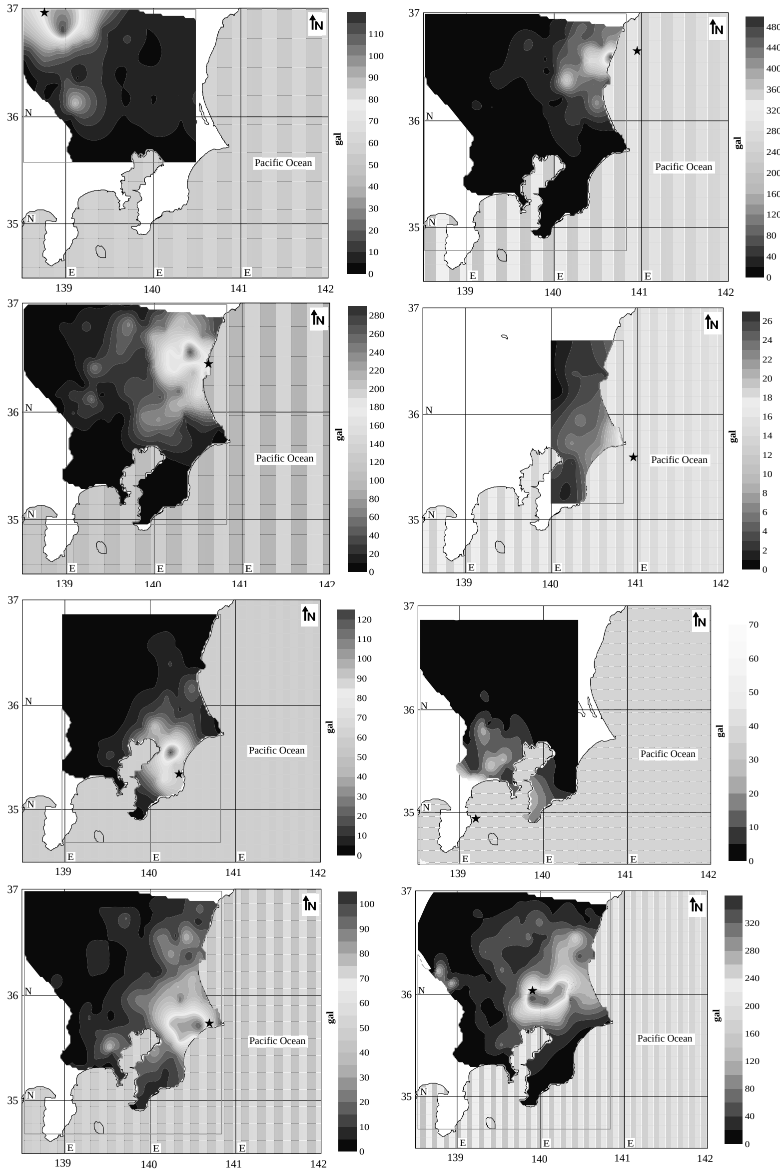

Fig (15): Contour map illustrating the attenuation characteristic distribution of the actual PGA of each of the selected eight earthquakes in the Kanto region.

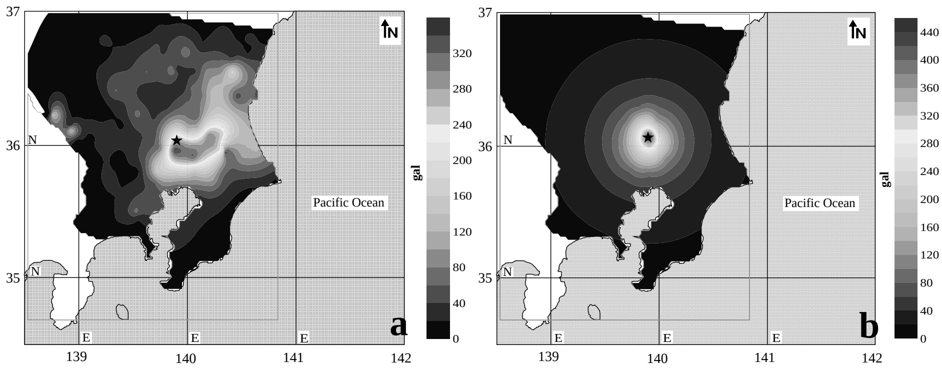

Fig (16): (a) Contour map illustrating the actual PGA attenuation characterisation. (b) Contour map illustrating the estimated maximum PGA attenuation characterisation for the 2005-02-16 earthquake.

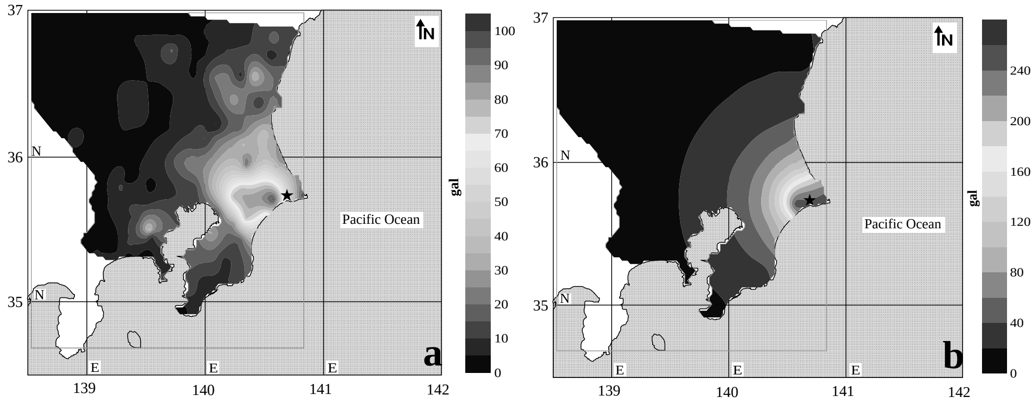

Fig (17): (a) Contour map illustrating the actual PGA attenuation characterisation. (b) Contour map illustrating the estimated maximum PGA attenuation characterisation for the 2005-06-20 earthquake.

Estimating the ground motion, either implicitly through the use of special earthquake codes or more specifically via site-specific investigations, is essential for designing engineered structures. The development of design criteria requires, at a minimum, a strong-motion attenuation relationship to estimate the earthquake ground motions from specific parameters characterising the earthquake source, geologic conditions of the site, and length of the propagation path between the source and the site. Two earthquakes were selected to use, as typical examples for estimating PGA.

The maximum PGA is the most convenient way to calculate the value of the acceleration response spectrum as a function of distance and magnitude. In order to evaluate the average value, the influence and effect of the asperity rupture process was not considered separately. The distance attenuation formulas for maximum PGA in the top surface of a foundation engineering layer have been derived (Eqs. 2) (Shi and Midorikawa, 1999).

$$\log PGA = 0.50Mw + 0.0043D + 0.61 - \log(X + 0.0055\times100.5Mw) - 0.003X \quad (2)$$

where: PGA is the maximum peak ground acceleration (gal), Mw is the moment magnitude, D is the focal depth (km), and X is the minimum distance (km).

The maximum PGA was calculated using the formulas derived by Shi and Midorikawa, (1999) for the two selected typical earthquakes (Figs. 16 and 17). The maximum estimated PGA attenuation characterisations displayed relative matching with the actual PGA, with concentric shape and small coverage area related to the homogenous medium assumption of Shi and Midorikawa, (1999) derived equation. However, the actual PGA attenuation characterisations appeared as semi-elongated shapes with large coverage areas affected with the heterogeneous medium and lateral changes in Vs30 values.

SUMMARY AND CONCLUSIONS

Using 58 boreholes at KiK-net, for which the velocity model extends to at least 30 m, we investigated several methods for extrapolating Vs to 30 m. Methods using the statistical properties of the relationship between Vs(30) and the simple method of assuming that, the lowermost velocity extends to 30 m resulted in significantly less bias than did shallower extrapolated velocities for shallow models. In addition, for all methods, the percentage of sites misclassified was generally less than 10%. The results suggest that, determining site classes might prove useful for any datasets, such as the K-NET and KiK-net datasets or other sites, through which shear-wave velocity models might extend to depths significantly less than 30 m (such as many seismic cone penetrometer soundings).

The results could also consider geological information, such as whether the site is expected to be underlain to 30 m by Holocene materials alone, Pleistocene materials alone, or some combination. As such, the analysis is dominated by NEHRP class B to E sites. Classes B and C were found to most closely match with the mountainous areas on the northern and north-western sides of the Kanto region, but class D spread across most areas of the Kanto basin. The fourth class, E, related to soft soil materials, was associated with low average shear velocity sites due to the weak lithologic units (loose sand and silt, very soft clay, and organic soil) recorded at these areas and described during the drilling process.

The calculated site amplification factor in the Kanto region is ranged between 0.4 and 4.97. High site amplification factor corresponds to zones with relatively thick sedimentary thicknesses, relatively low values of average shear-wave velocity, and low NEHRP site class orders (class D and E), and changes to relatively low values in the mountainous areas.

Finally, we compared the maximum PGA for two selected earthquakes as examples and compared them with the actual PGA. The comparison revealed that, the maximum estimated PGA attenuation characterisations display relative matching with the actual PGA, with concentric shapes and small coverage areas related to a homogenous medium assumption of the derived equation used in the estimation. However, the actual PGA attenuation characterisations appear as a semi-elongated shape with large coverage areas affected with the heterogeneous media and lateral changes in Vs(30) values.

REFERENCES

Aki, K., (1988): Local site effects on strong ground motion, Proc. Earthquake Eng. Soil Dyn. II, 103-155.

Aki, K., and Irikura, I., (1991): Characterization and mapping of earthquake shaking for seismic zonation, Proc. of the 4th International Conference on Seismic Zonation, 1, Stanford, California, 61-110.

Bard, P.-Y., (1994): Effects of surface geology on ground motion: recent results and remaining issues, Proc. of the l0th European Conference on Earthquake Eng., t, 305-325.

Boore, D.M., (2004): Estimating Vs(30) (or NEHRP Site Classes) from shallow velocity models (Depth < 30 m), Bulletin of Seismological Society of America, Vol.94, No.2, 591-597.

Boore, D.M., Joyner, W.B., and Fumal, T.E., (1997): Equations for estimating horizontal response spectra and peak acceleration from western North American earthquakes: a summary of recent work, Seism. Res. Lett. 68, 128–153.

Borcherdt, R.D., and Gibss, J.F., (1976): Effects of local geological conditions in the San Francisco bay region on ground motions and the intensities of the 1906 earthquake, Bulletin of Seismological Society of America, Vol.66, No.2, 467-500.

Building Seismic Safety Council (BSSC), (2001): NEHRP recommended provisions for seismic regulations for new buildings and other structures, 2000 Edition, Part 1: Provisions, prepared by the Building Seismic Safety Council for the Federal Emergency Management Agency (Report FEMA 368), Washington, D.C.

Building Seismic Safety Council (BSSC), (2003): The 2003 HEHRP Recommended Provisions for the Development of Seismic Regulations for New Buildings and Other Structures, FEMA, Washington D. C.

Campbell K., (1985): Strong motion attenuation relations: a ten-years perspective. Earthq Spectra, 71, 2039–2070

Dobry, R., Borcherdt, R.D., Crouse, C.B., Idriss, I.M., Joyner, W.B., Martin, G.R., Power, M.S., Rinne, E.E., and Seed, R.B., (2000): New site coefficients and site classification system used in recent building seismic code provisions, Earthquake Spectra, 16, 41–67.

Fujimoto, K., and Midorikawa, S., (2003): Average shear-wave velocity mapping throughout Japan using the Digital National Land Information, J. Japan Association for Earthquake Engineering, Vol. 3, No. 3, 13-27 (in Japanese with English abstract).

Fujimoto, K., and Midorikawa, S., (2006): Relationship between Average Shear-Wave Velocity and Site Amplification Inferred from Strong Motion Records at Nearby Station Pairs, Journal of Japan Association for Earthquake Engineering, Vol. 6, No.1, 11-22 (in Japanese with English abstract).

International Code Council, ICC, (2006): International Building Code. Structural and fire-safety provisions (seismic, wind, accessibility, egress, occupancy and roof codes), Whittier, CA.

Ishida, M., (1992): Geometry and relative motion of the Philippine Sea plate and Pacific plate beneath the Kanto-Tokai district, Japan, J. Geophys. Res., 97, 489–513.

Joyner, W.B., and Fumal, T.E., (1984): Use of measured shear-wave velocity for predicting geologic and site effects on strong ground motion, Proc. 8th World Conference on Earthquake Engineering, Vol. 2, 777-783.

Kanno, T., Narita, A., Morikawa, N., Fujiwara, H., and Fukushima, Y., (2006): A new attenuation relation for strong ground motion in Japan based on recorded data, Bull. Seism. Soc. Am., Vol. 96, No. 3, 879-897.

Kinoshita, S., Kyoshin Net (K-NET) (1998): Seism. Res. Letters, 69, 309-332.

Koketsu, K., and Higashi, S., (1992): Three-dimensional topography of the sediment/basement interface in the Tokyo metropolitan area, central Japan. Bull. Seism. Soc. Am., 82, 2328-2349.

Komazawa, M., and Hasegawa, I., (1988): The graben structure suggested by gravimetric basement in the Kanto district, central Japan. Mem. Geol. Soc. Japan, No. 31, 57-74.

Matsuoka, M., Wakamatsu, K., Fujimoto, K., and Midorikawa, S., (2006): Average shear-wave velocity mapping using Japan engineering geomorphologic classification map, Structural Eng./ Earthquake Eng., JSCE, Vol. 23, No. 1, 57s-68s.

Matsumura, S., (1997): Focal zones of a future Tokai earthquake inferred from the seismicity pattern around the plate interface, Tectonophysics, 273, 271-291.

Midorikawa, S., Matsuoka, M. and Sakugawa, K., (1994): Site effects on strong-motion records observed during the 1987 Chiba-ken-tohooki, Japan earthquake, Proc. 9th Japan Earthquake Engineering Symposium, Vol. 3, 85-90.

Noguchi, S., (2002): Earthquake clusters in the Kanto and Tokai subduction zones: implications for models of plate consumption, Seismotectonics in Convergent Plate Boundary, Eds, Y. Fujinawa and A. Yoshida, 451-467.

Okada, Y., and Kasahara, K., (1990): Earthquake of 1987, off Chiba, central Japan and possible triggering of eastern Tokyo earthquake of 1988, Tectonophysics, 172, 351–364.

Seno, T., Stein, S., and Gripp, A.E., (1993): A model for the motion of the Philippine Sea plate consistent with NUVEL-1 and geological data, J. Geophys. Res., 98, 17941-17948.

Seno, T., Sakurai, T., and Stein, S., (1996): Can the Okhotsk plate be discriminated from the North American plate?, J. Geophys. Res., 101, 11305-11315.

Si, S., and Midorikawa, S., (1999): New attenuation relationships for peak ground acceleration and velocity considering effects of fault type and site condition, Journal of Structural and Construction Engineering (Transaction of AIJ), 523, 63-70 (in Japanese with English abstract).

Smith, W.H., and Sandwell, D.T., (1997): Global sea floor topography from satellite altimetry and ship depth soundings, Science, 277, issue 5334.

Suzuki, H., (2002): Underground geological structure beneath the Kanto Plain, Japan. Rep. Nat. Res. Inst. Earth Sci. Disaster Prevention, No. 63, 1-19.

Wills, C.J., Petersen, M., Bryant, W. A., Reichle, M., Saucedo, G. J., Tan, S., Taylor, G., and Treiman, J., (2000): A site-conditions map for California based on geology and shear-wave velocity, Bull. Seism. Soc. Am., 90, S187–S208.

Yamanaka, H., and Yamada, N., (2002): Estimation of 3D S-wave velocity model of deep sedimentary layers in Kanto plain, Japan, using microtremor array measurements. Butsuri-Tansa, 55, 53-65.

Yamanaka, H., and Yamada, N., (2005): Construction of 3D S-wave velocity model of the Kanto basin, Japan, using Rayleigh wave phase velocity. 2nd International Workshop, Strong Ground Motion Prediction and Earthquake Tectonics in Urban Areas, October 25-27, at Earthquake Research Institute, University of Tokyo, Japan,107-112.